

Contract No:

This document was prepared in conjunction with work accomplished under Contract No. DE-AC09-08SR22470 with the U.S. Department of Energy (DOE) Office of Environmental Management (EM).

Disclaimer:

This work was prepared under an agreement with and funded by the U.S. Government. Neither the U. S. Government or its employees, nor any of its contractors, subcontractors or their employees, makes any express or implied:

- 1) warranty or assumes any legal liability for the accuracy, completeness, or for the use or results of such use of any information, product, or process disclosed; or
- 2) representation that such use or results of such use would not infringe privately owned rights; or
- 3) endorsement or recommendation of any specifically identified commercial product, process, or service.

Any views and opinions of authors expressed in this work do not necessarily state or reflect those of the United States Government, or its contractors, or subcontractors.



**Savannah River
National Laboratory®**

A U.S. DEPARTMENT OF ENERGY NATIONAL LABORATORY • SAVANNAH RIVER SITE • AIKEN, SC

Porous Membranes for Moisture Probe Protection (SR18024)

Kaitlin Lawrence

Paul Beaumont

Donna Allison

Jeffrey Steedley

September 19, 2020

SRNL-STI-2020-00403, Revision 0

SRNL.DOE.GOV

DISCLAIMER

This work was prepared under an agreement with and funded by the U.S. Government. Neither the U.S. Government or its employees, nor any of its contractors, subcontractors or their employees, makes any express or implied:

1. warranty or assumes any legal liability for the accuracy, completeness, or for the use or results of such use of any information, product, or process disclosed; or
2. representation that such use or results of such use would not infringe privately owned rights; or
3. endorsement or recommendation of any specifically identified commercial product, process, or service.

Any views and opinions of authors expressed in this work do not necessarily state or reflect those of the United States Government, or its contractors, or subcontractors.

Printed in the United States of America

**Prepared for
U.S. Department of Energy**

Keywords: *Moisture Probe*
Semi-permeable membranes

Retention: *Varies*

Porous Membranes for Moisture Probe Protection (SR18024)

Kaitlin Lawrence
Paul Beaumont
Donna Allison
Jeffrey Steedley

September 19, 2020

Prepared for the U.S. Department of Energy under
contract number DE-AC09-08SR22470.



REVIEWS AND APPROVALS

AUTHORS:

Kaitlin Lawrence, Nonproliferation Technology Date

Paul Beaumont, Hydrogen Isotope Process Science Date

Donna Allison, Hydrogen Isotope Process Science Date

Jeffrey Steedley, Hydrogen Isotope Process Science Date

TECHNICAL REVIEW:

George K. Larsen, Hydrogen Isotope Process Science Date

APPROVAL:

Heather Mentzer, Project Co-lead, Process & Shift Engineering Date

Paul Foster, PDRD Program Manager, Process & Shift Engineering Date

Patterson Nuessle, Manager Date
Nonproliferation Technology

ACKNOWLEDGEMENTS

The authors would like to acknowledge Esther Kent for her contributions to this work during her summer internship in the summer of 2018. The authors would also like to acknowledge George Larsen and Tommy Sessions for their input and guidance in this work. This project was funded by the Savannah River Tritium Enterprise Plant Directed Research and Development program under project number SR18024.

EXECUTIVE SUMMARY

In the presence of contaminants, moisture probes can give false moisture readings and have shorter lifetimes. Absolute humidity probes are composed of porous, hygroscopic metallic oxide thin films (Al_2O_3) coupled to electrodes (e.g. Au and Al). While these materials provide absolute humidity readings at low water levels at a relatively low cost, they are sensitive to the presence of contaminants, especially ammonia, due to its high hygroscopicity and ability to bind to the probe.¹ Without frequent recalibration, especially in the presence of contaminants, the humidity levels are inaccurately reported due to measurement drift that occurs when the pores close, changing the impedance of the probe.² The goal of this project was to improve the stability and reliability of these moisture probes by incorporating a molecular sieve into the probe to allow only the water to reach the sensor. Molecular sieves contain pores that allow molecule specific permeation. Two dimensional inorganic nanosheets (e.g. BN, MoO_2 , MoS_2) have recently been shown to behave as molecular sieves for water.³ Compared to zeolites, nanoporous materials have higher flux rates through the pores, leading to faster water permeation.³ Graphene oxide sheets have also been successfully employed for unimpeded water permeation; however, at lower humidity levels, the structure is unstable and the pores shrink, preventing the sieving of molecules. Compared to graphene oxide, sheets based off of inorganic materials, such as molybdenum, have been found to be more stable at lower humidity levels and have faster permeation rates.³ By creating a barrier in front of the Al_2O_3 sensor chip to prevent the permeation of contaminants into the probe, the lifetime of the probe will be extended. While the molybdenum sheets are a promising material for this application, their performance against ammonia and tritiated compounds have not yet been evaluated. This technology can be applied to other applications, including gas and liquid purification for environmental remediation, single molecule sensors, field effect transistors, and catalysts.

TABLE OF CONTENTS

LIST OF TABLES	viii
LIST OF FIGURES	viii
LIST OF ABBREVIATIONS.....	ix
1.0 Introduction.....	1
2.0 Experimental Procedure.....	2
2.1 Materials.....	2
2.2 Membrane Fabrication	2
2.3 Characterization.....	3
2.4 Gas Permeation.....	3
3.0 Results and Discussion	4
3.1 Initial GO membrane studies.....	4
3.2 Investigation of other membranes	8
3.3 Low Ammonia Permeation Studies.....	11
3.4 Ammonia Desorption	11
4.0 Conclusions.....	13
5.0 Recommendations, Path Forward or Future Work	13
6.0 References.....	14
Appendix A	15

LIST OF TABLES

No table of figures entries found.

LIST OF FIGURES

Figure 1-1. Mechanism of gas permeation through layered membranes	1
Figure 1-2. (a) Mechanisms for membrane separation and transport mechanisms; (b) Structure and thickness of common membrane types ⁵	2
Figure 3-1. (a) XRD (b) AFM and (c) a picture of graphene oxide membrane	4
Figure 3-2. Nitrogen permeability for GO filter compared to uncoated (blank) filter paper with error bars for the standard deviation	5
Figure 3-3. Effect of membrane thickness on the permeability of nitrogen through the membrane	6
Figure 3-4. Effect of molecular weight on gas permeability: (a) permeability as a function of pressure for the different gases; (b) effect of pressure on the permeability.....	6
Figure 3-5. Ammonia water permeation for GO membranes: (a) RGA spectra downstream of the membrane and (b) ammonia partial pressure (m/z 17) for the different GO thicknesses	7
Figure 3-6. Effect of ammonia permeation on GO membranes (a) Nitrogen permeability and (b) FTIR before and after ammonia permeation	8
Figure 3-7. Nitrogen permeability for membranes composed of different membranes.....	9
Figure 3-8. FTIR of (a) BN and (b) MoS ₂ after ammonia permeation	9
Figure 3-9. Ammonia water permeation for MoO ₃ based membranes: (a) RGA spectra downstream of the membrane and (b) ammonia partial pressure (m/z 17) for the different membrane thicknesses	10
Figure 3-10. SEM of MoO ₃ membranes before (a) and after (b) ammonia permeation with EDX (inset) 10	
Figure 3-11. RGA Calibration curve for ammonia	11
Figure 3-12. TPD for GO (a) as is and (b) with ammonia	12
Figure 3-13. TPD for BN (a) as is and (b) with ammonia	12
Figure 3-14. TPD for MoS ₂ (a) as is and (b) with ammonia.....	13

LIST OF ABBREVIATIONS

A	Membrane area
AFM	Atomic Force Microscopy
ATR	Attenuated Total Reflectance
BN	Boron Nitride
δ	Membrane thickness
FTIR	Fourier Transform Infrared Spectroscopy
GO	Graphene Oxide
MS	Mass Spectrometer
m/z	Mass to charge ratio
P_a	Permeability
Q	Mass flow rate
RGA	Residual Gas Analyzer
SRNL	Savannah River National Laboratory
TPD	Temperature Programmed Desorption
XRD	X-Ray Diffraction

1.0 Introduction

Aluminum based moisture probes are sensitive to contaminants and can read erroneously when contaminants bind to the probes surface and change the impedance.¹ To prevent unwanted species from binding to the moisture probe, a membrane that prevents the permeation of other polar (non-water) molecules from reaching the moisture probe can extend the lifetime of the probe and reduce the need for frequent calibrations, leading to cost savings. The goal of this project is to create a membrane that protects the moisture probe from contaminants, such as ammonia. Ideally, the membrane will selectively allow water permeation over ammonia at low moisture levels. Two dimensional layered materials that have lamellar architecture, such as graphene and graphene oxide, are currently the most studied materials for selective gas permeation.⁴ These materials restrict flow by creating a tortuous path for gas molecules through the pores and interlayer diffusion (Figure 1-1).⁵ Graphene based membranes also have high mechanical strength and chemical robustness, along with minimal material thickness, making them ideal candidates for membrane based separation mechanisms.⁵

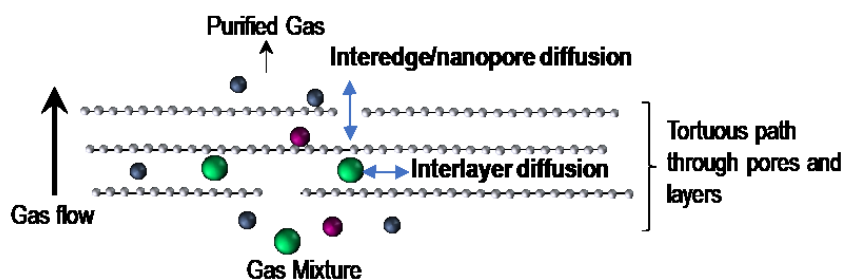


Figure 1-1. Mechanism of gas permeation through layered membranes

The pore size and layer structure of inorganic two-dimensional materials allow for the separation of molecules based on size and chemical affinity for the pores. In nanoporous membranes, the separation can occur through molecular sieving or Knudsen diffusion depending on the pore size and layer thickness (Figure 1-2).⁵ For graphene, thinner membranes lead to an increase in permeation selectivity. Atomically thin graphene membranes are impermeable to gases and have been found to hold pressure, essentially acting like a one layer thick balloon.⁶ Physicochemical effects, such as steric effects, chemical functionalities, surface charges and dielectric effects, also plays a role in the separation and adsorption of gas species.

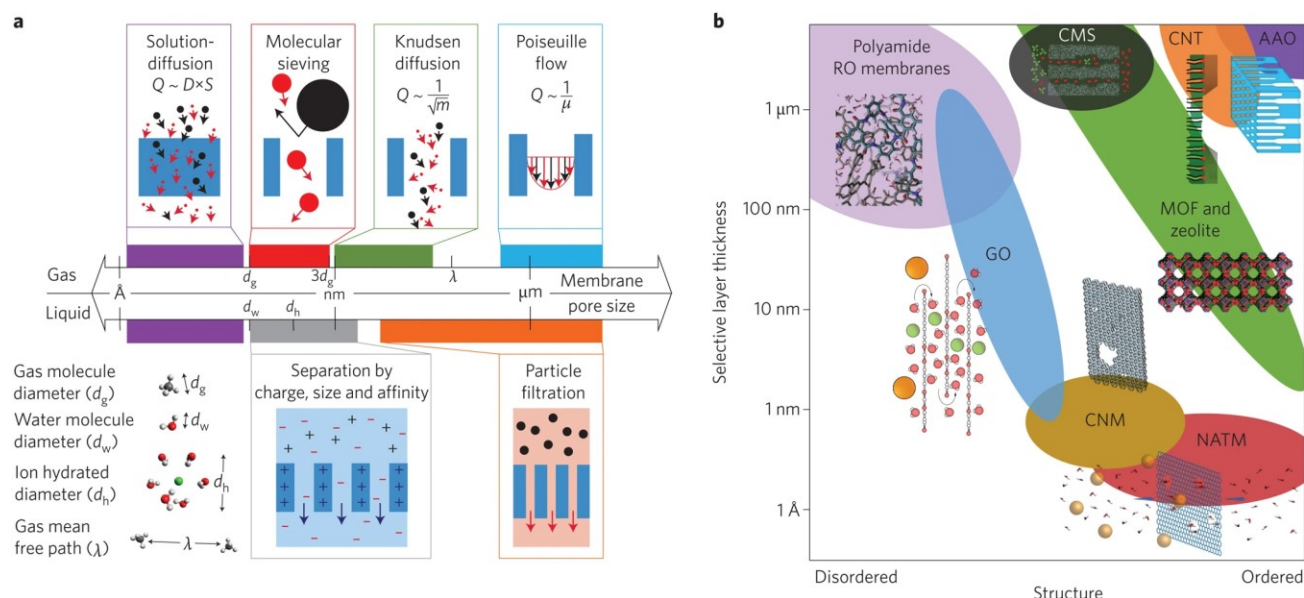


Figure 1-2. (a) Mechanisms for membrane separation and transport mechanisms; (b) Structure and thickness of common membrane types⁵

While graphene-based materials have shown a lot of promise in gas separation applications, they have low permeability of water, especially in low humidity due to the collapse of the 2D structure. To overcome this, other more hydrophilic two-dimensional structures, such as MoS₂ and boron nitride (BN) have been investigated.⁷ Literature reports on molybdenum and other inorganic based two dimensional membranes have shown lower energy barriers for water permeation compared to graphene membranes because of their higher hydrophilicity.³ The permeation of ammonia through molybdenum and boron membranes has not been investigated previously. In this project, different membranes were created and their performance in gas streams with ammonia was measured. The effect of membrane morphology and ammonia concentration on the membrane's performance was measured.

2.0 Experimental Procedure

2.1 Materials

Materials were purchased and used without further purification. Single layer graphene oxide (GO) was purchased from Graphene Supermarket, Whatman anodisc filter membranes (d=47 mm, porosity=0.47 μm) were purchased from Sigma Aldrich.

2.2 Membrane Fabrication

Aqueous solutions of the membrane material (0.1 mg/mL) were sonicated for 12-14 hours. The solution was vacuum filtered onto Whatman filters membranes and dried in an oven at 50 °C for 24 hours.

2.3 Characterization

Residual Gas Analyzer (RGA): RGA measurements were carried out on a Dycor Ametek LD 100 Mass Spectrometer equipped with a faraday cup detector and a T-station 85 turbomolecular pumping station from Edwards vacuum.

X-Ray Diffraction (XRD): XRD measurements were taken using X-ray diffractometer (PANalytical PW3040-PRO) using monochromatic Cu-K α X-ray radiation ($\lambda = 1.5418 \text{ \AA}$) generated from a copper anode supplied with 40 kV and a current of 40 mA. Data were collected over a range of 5-80° 2 θ with a step size of 0.01°. Background spectra of the filter paper and sample holder were collected and subtracted from the raw XRD data. The average d-spacing was calculated using Bragg's Law (eq. 1), where λ is the wavelength of the X-ray source, d is the interplanar distance and θ is the glancing angle as measured by the XRD.

$$\lambda = 2d\sin\theta \quad (1)$$

Fourier Transform Infrared Spectroscopy (FTIR): Spectra were measured using a Jasco 6300 FT/IR with an Attenuated Total Reflectance (ATR) accessory equipped with a ZnSe crystal. The measurements were carried out in N₂ atmosphere using a DTGS detector.

Atomic Force Microscopy (AFM): AFM measurements were carried out

Temperature-Programmed-Desorption (TPD): TPD analyses were performed using a Micromeritics AutoChem II 2920 with an MKS Cirrus mass spectrometer (MS), using an ionization energy of 40 eV. Experimental conditions heated the sample to 700 °C at a rate of 10 °C/min. Prior to TPD analysis, samples were treated with anhydrous ammonia using flow-through reactors created in-house to induce saturation.

2.4 Gas Permeation

Gas permeation was performed using a constant volume pressure method with feed pressures 800-2000 Torr. Membranes were placed in a stainless-steel membrane holder and gases were measured using mass flow controllers and pressure transducers. The manifold was equipped with a bubbler to introduce a saturated water vapor stream through the membrane. The permeability was calculated using the Barrer equation (eq. 2).

$$P_a = \frac{1}{\Delta P} \times \frac{\delta}{A} \times Q \quad (2)$$

Where P_a is the permeability in Barrer, ΔP is the difference between the upstream and downstream pressures, δ the membrane thickness, A is the membrane area, and Q is the mass flow rate through the membrane.

3.0 Results and Discussion

3.1 Initial GO membrane studies

Membranes were fabricated from aqueous solutions and vacuum filtered onto filter paper supports. They were characterized using XRD, AFM, and FTIR. As shown in Figure 3-1, a peak in the XRD around 12.5 was measured for graphene oxide (GO) membranes, corresponding to an interlayer distance of 6.85 Å. The membrane was transferred onto a flat, silicon wafer and measured using AFM to determine the membrane thickness, which was measured to be 0.96 μm, corresponding to about 1000 GO layers.

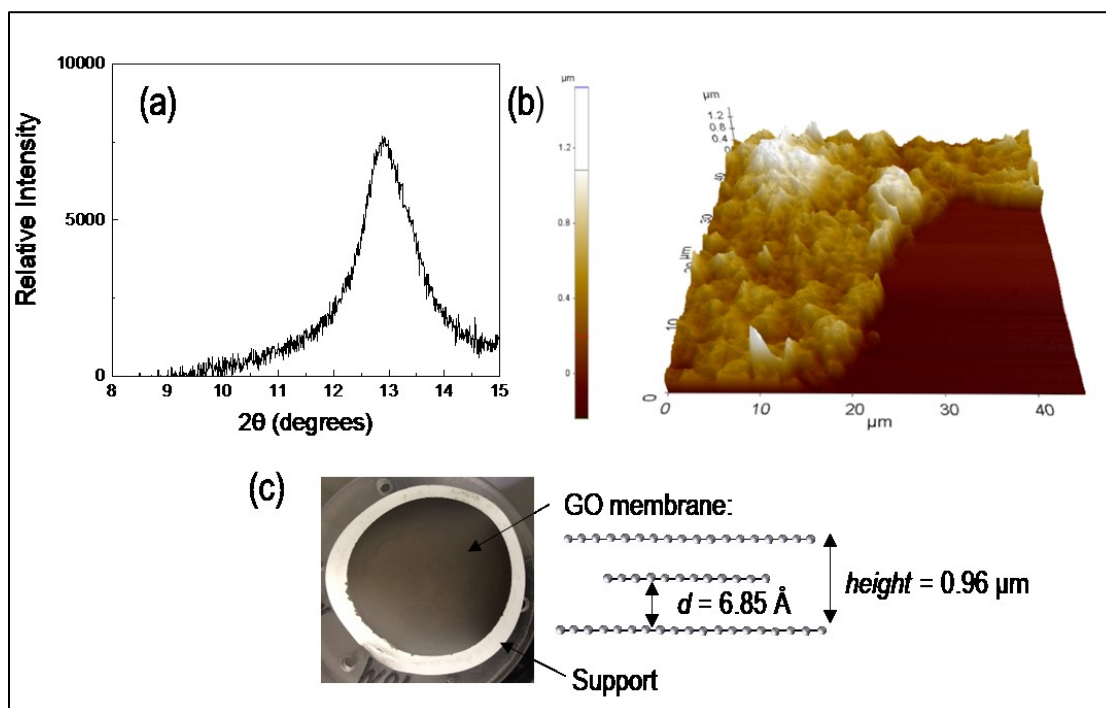


Figure 3-1. (a) XRD (b) AFM and (c) a picture of graphene oxide membrane

For permeability measurements, the filter papers were cut so that the entire surface of the filter paper that was in the flow path was functionalized. The GO filters showed a decrease in permeability compared to the uncoated filter paper (Figure 3-2). The functionalized filter paper had a higher permeability at a feed pressure of 800 Torr but, after 1200 Torr, there is minimal effect on permeability from the feed pressure. This was also observed in the unfunctionalized membrane control (Figure A-1). This may be due to a flow drop in the manifold resulting from flow restriction because of the inner diameter of the 1/16" tubing. Compared to the blank control, the permeability of the membrane is lower, resulting from the membrane deposition.

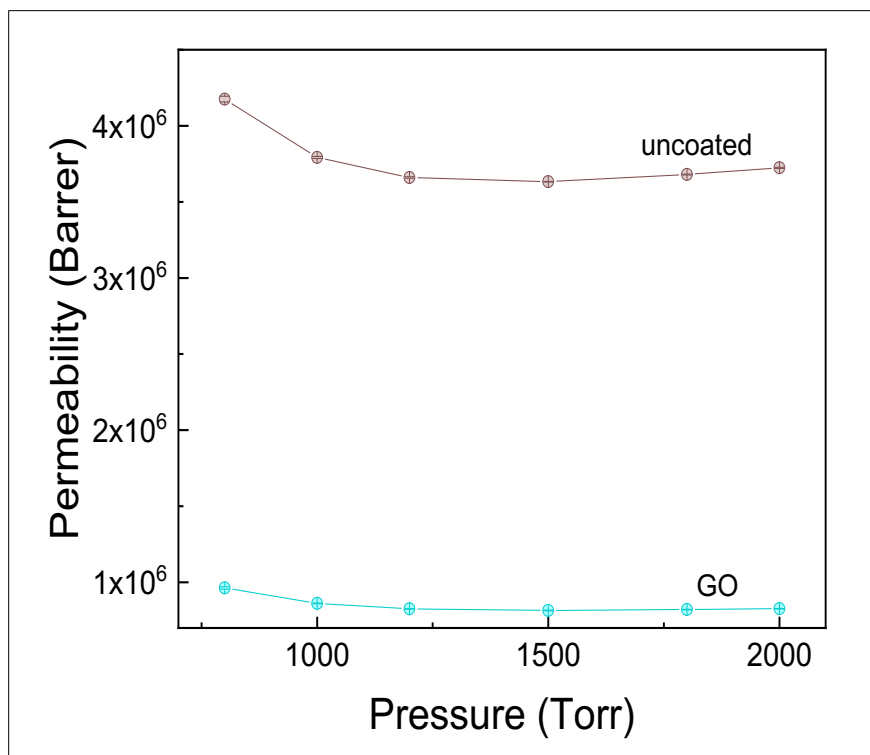


Figure 3-2. Nitrogen permeability for GO filter compared to uncoated (blank) filter paper with error bars for the standard deviation

The thickness of the GO membranes was controlled by changing the concentration of the GO that was deposited onto the filter support. Thicker GO membranes had a higher permeability for nitrogen through the support (Figure 3-3). This is consistent with other membrane studies and the Barrer equation (eq. 2).⁸⁻⁹ The membranes used in these experiments were fabricated through vacuum filtration, leading to weaker interlayer spacing compared to other methods such as chemical vapor deposition.⁴ As the number of layers increases, the interlayer spacing increases, leading to higher gas permeance with increased thickness, indicating the gas transport is mostly dependent on the interlayer spacing.

The size of the gas molecule also had an effect on gas permeance and followed the trend typically found with Knudsen diffusion mechanism, where permeance decreased with increasing molecular weight (Figure 3-4b and Figure 3-5).

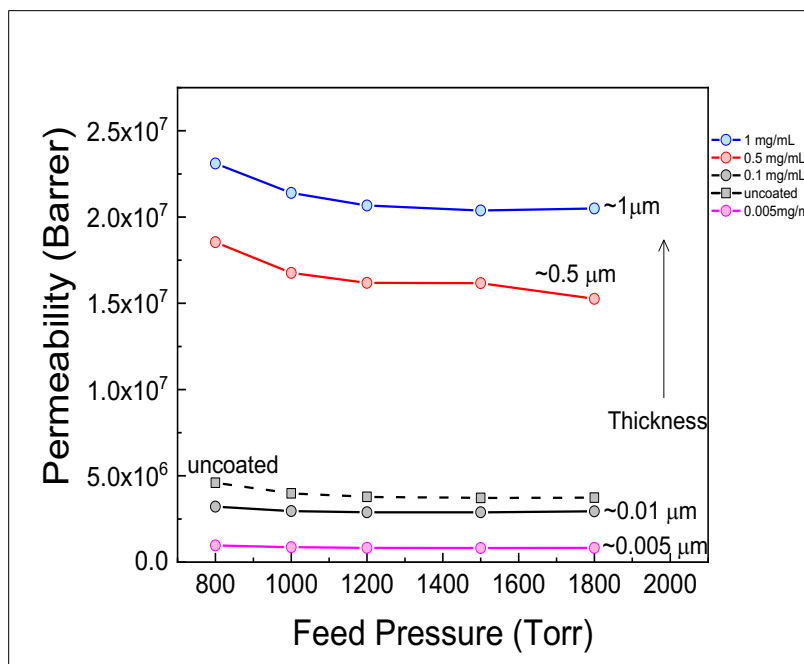


Figure 3-3. Effect of membrane thickness on the permeability of nitrogen through the membrane

The size effect on permeability was not significantly affected by upstream pressure (Figure 3-5), where a similar, slightly lower, permeability was measured at the higher pressure.

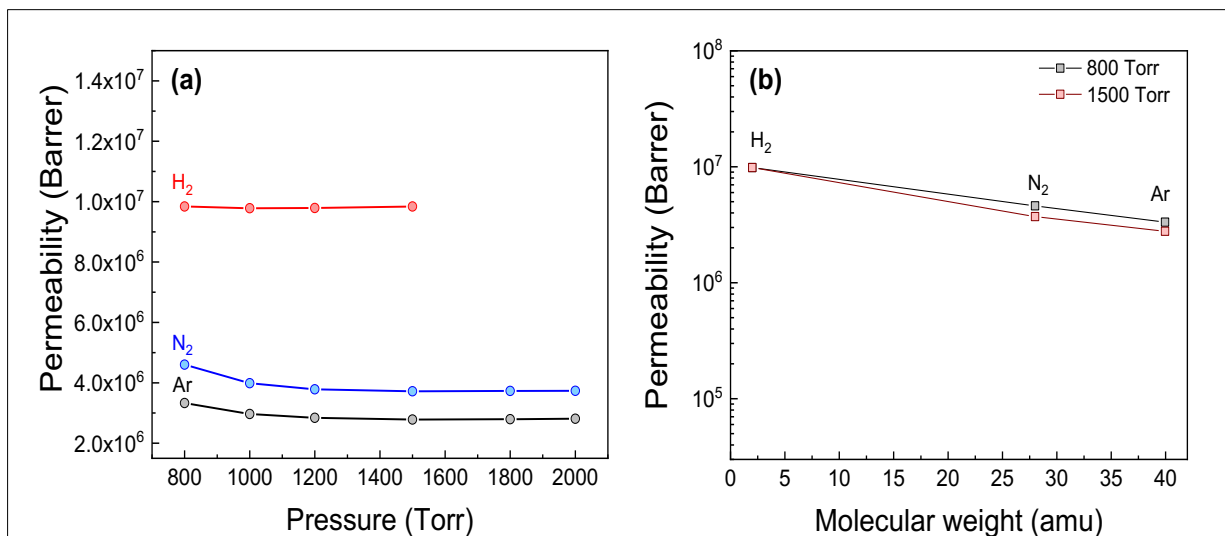


Figure 3-4. Effect of molecular weight on gas permeability: (a) permeability as a function of pressure for the different gases; (b) effect of pressure on the permeability

The effect of membrane thickness on ammonia and water permeation was measured for GO, as shown in Figure 3-5. The RGA signal was monitored at m/z 17, which has contributions from ammonia and water fragments. As shown in Figure 3-5a, the water signal did not decrease, but the ammonia fragments (m/z 15-17) decreased permeation. Therefore, m/z 17 was used to monitor the

ammonia levels and is assumed to make up most of the signal. A lower partial pressure for ammonia was measured on the outlet of the moisture probe for the thicker membranes.

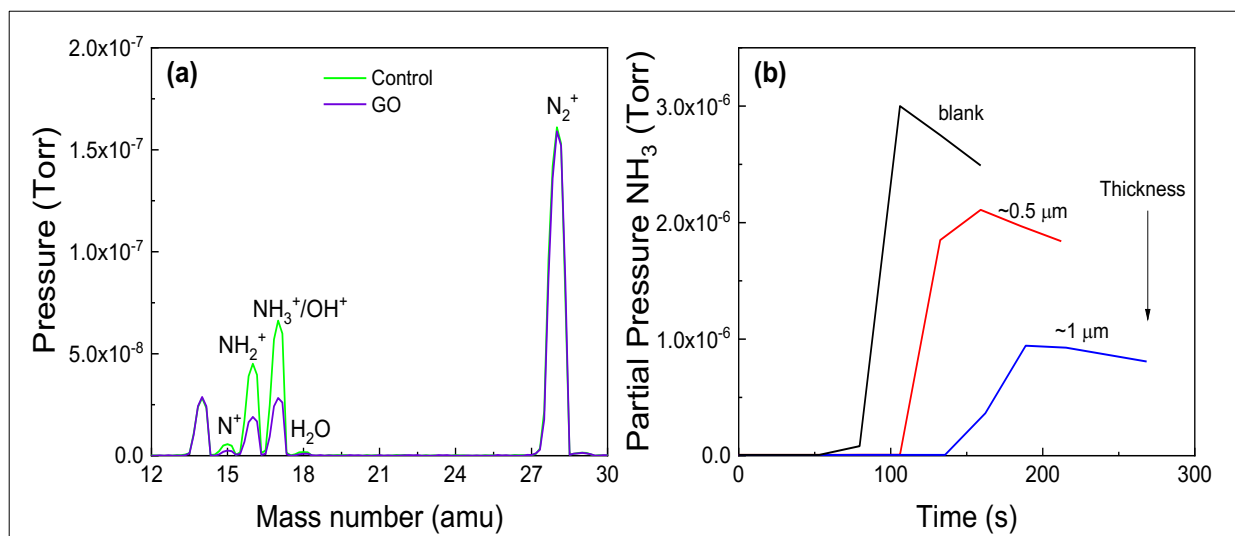


Figure 3-5. Ammonia water permeation for GO membranes: (a) RGA spectra downstream of the membrane and (b) ammonia partial pressure (m/z 17) for the different GO thicknesses

To measure the stability of the membranes after ammonia permeation, the nitrogen permeability was measured before and after ammonia permeation (Figure 3-6a). The permeability had slightly decreased after ammonia permeation which may be due to the pores closing and becoming impermeable; however, this effect is small. A control blank membrane did not have a decrease in permeation after ammonia (Figure A-2). In the FTIR spectra in Figure 3-6b, a peak for the N-H stretch appears after ammonia permeation, indicating ammonia is binding to the membrane. GO has surface hydroxyl groups that can bind to ammonia and remove it from the gas stream.

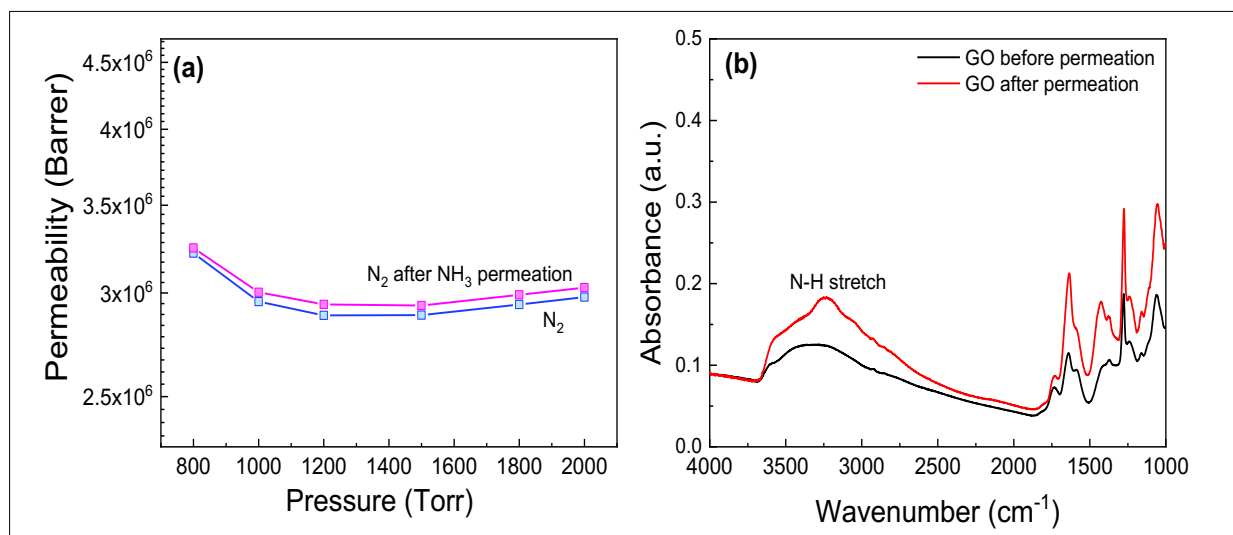


Figure 3-6. Effect of ammonia permeation on GO membranes (a) Nitrogen permeability and (b) FTIR before and after ammonia permeation

3.2 Investigation of other membranes

Other two-dimensional membranes were investigated, including boron nitride and molybdenum sulfide. These materials have a similar layering structure as GO but different hydrophilicities that will affect the amount of water that passes through the membrane. GO membranes are more hydrophobic and become impermeable to most gases as they move closer to single layer GO. At lower water levels, GO would prevent any moisture from reaching the moisture probe. As shown in Figure 3-7., the membranes have similar permeabilities for nitrogen, with MoS₂ showing the lowest permeation and BN showing the highest. Boron nitride is reported to have a higher pore size, 3.2 nm, compared to MoS₂ which is reported to have a pore size of 2.8 nm, so the higher permeation for BN is expected.

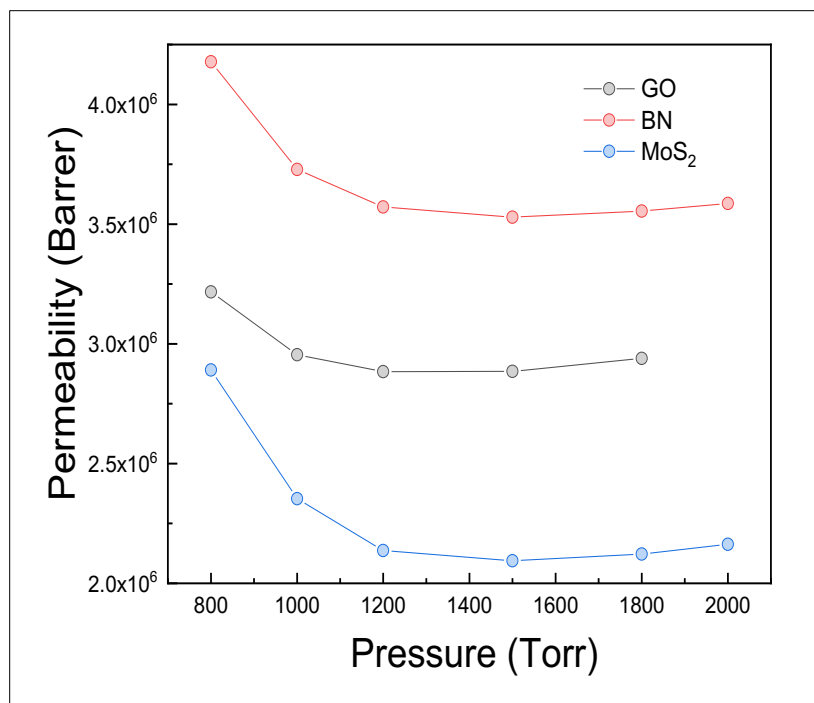


Figure 3-7. Nitrogen permeability for membranes composed of different membranes

The effects of ammonia permeation on the structure of the membranes was measured via FTIR before and after several cycles of ammonia permeation. As shown in Figure 3-8, the BN did not show a significant difference in the FTIR; however, a N-H stretch around 3500 cm⁻¹ for the MoS₂ appeared after ammonia permeation, indication ammonia adsorption is occurring.

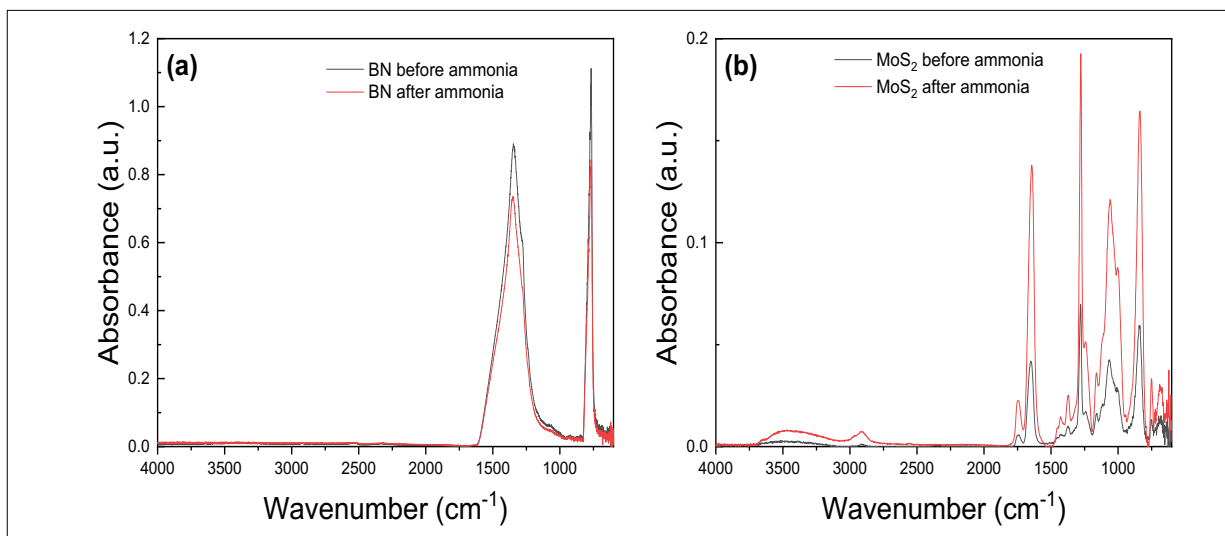


Figure 3-8. FTIR of (a) BN and (b) MoS₂ after ammonia permeation

Molybdenum oxide membranes were created from MoO₃ that was synthesized using standard wet chemical methods¹⁰ and the permeation was measured (Figure A-3.). Similar to the GO membrane, the RGA measured a lower partial pressure of ammonia on the outlet of the membrane; however, more ammonia appears to have permeated through the membrane than compared to the GO membranes, as indicated by a smaller decrease in the signal (Figure 3-9).

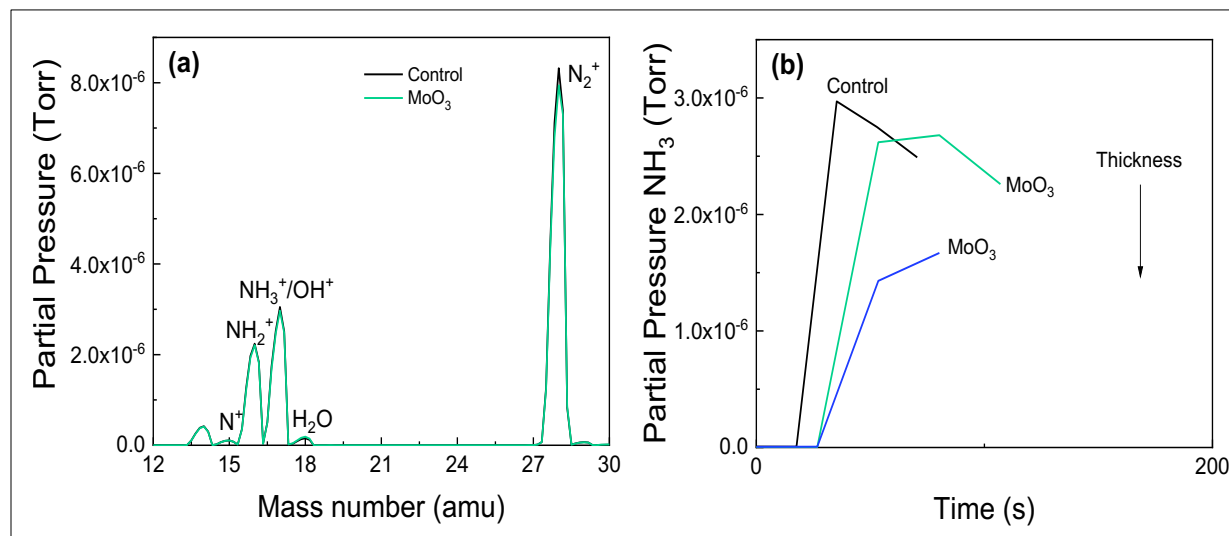


Figure 3-9. Ammonia water permeation for MoO₃ based membranes: (a) RGA spectra downstream of the membrane and (b) ammonia partial pressure (m/z 17) for the different membrane thicknesses

SEM/EDX of the membranes before and after ammonia permeation (Figure 3-10) were measured. The EDX for the MoO₃ membrane after ammonia permeation (Figure 3-10b inset) show a nitrogen peak, corresponding to the adsorption of ammonia in the membrane.

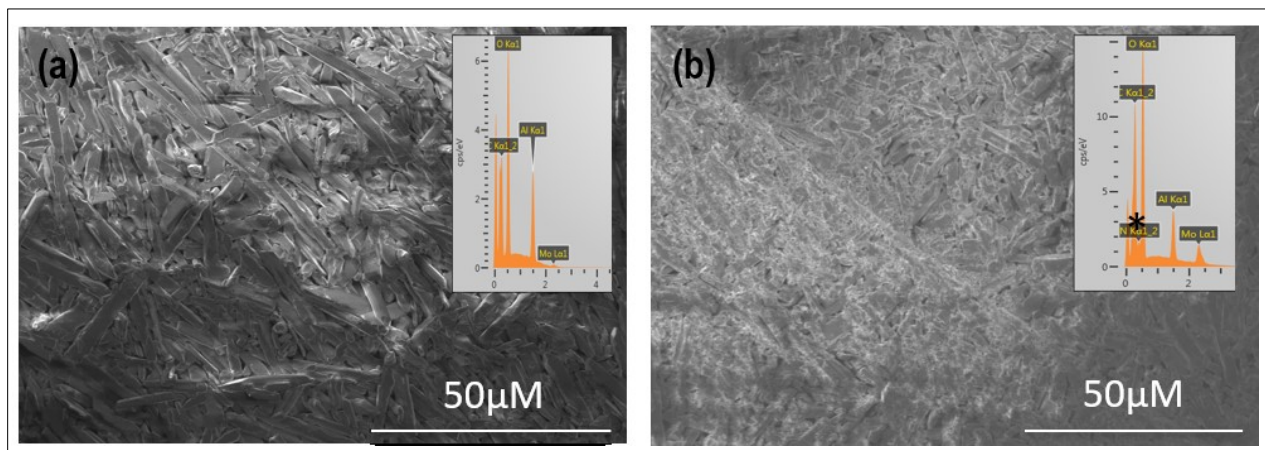


Figure 3-10. SEM of MoO₃ membranes before (a) and after (b) ammonia permeation with EDX (inset)

3.3 Low Ammonia Permeation Studies

The ammonia permeation was investigated systematically with increasing ammonia concentration. At increasing ammonia concentration, the ammonia concentration for the GO membrane was about 12% lower than for the blank run. This indicates that even at lower ammonia concentrations, the GO membrane is preventing ammonia permeation, either through adsorption or size exclusion.

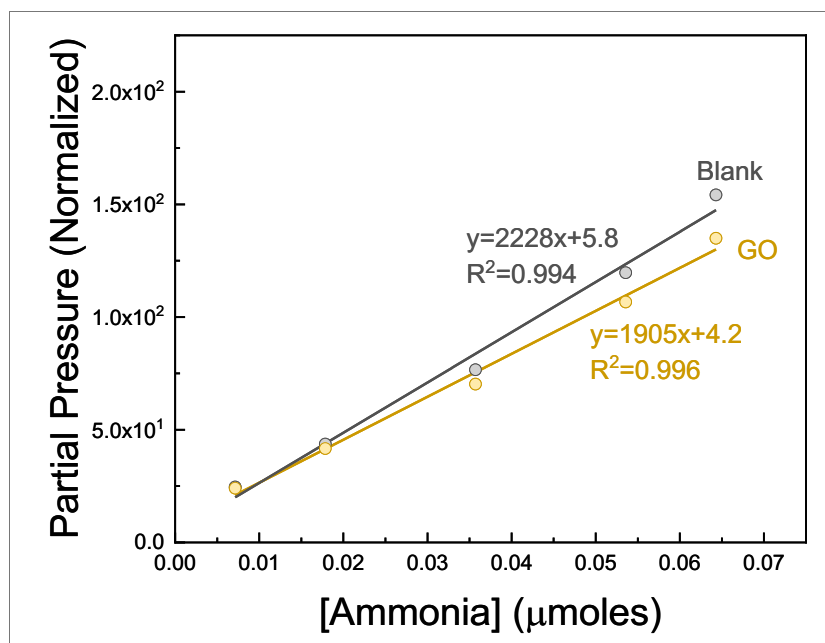


Figure 3-11. RGA Calibration curve for ammonia

3.4 Ammonia Desorption

To investigate the ammonia binding to the membranes, temperature programmed desorption (TPD) experiments were carried out for GO (Figure 3-12), BN (Figure 3-13) and MoS₂ (Figure 3-14). The membranes all appear to have a water peak around 100 °C in the samples without ammonia due to the weakly bound surface water. The GO sample also showed a spike in the signals at 160 °C, which was reproducible (Figure A-4). This may be due to the GO absorbing a large amount of ammonia, which appears to have a wide range of chemisorption interactions based on the broad desorption profiles from around 50 °C to 300 °C with a steep drop off after 350 °C. MoS₂ appeared to have the second strongest interaction with ammonia and water, with water and ammonia desorbing around 300 °C with another peak for water around 400 °C, as expected since MoS₂ is the most hydrophilic of the membranes. BN appears to have a broad water desorption peak around 600 °C which could be due to strongly bound water in the surface. These data indicate the strength of ammonia binding to the membrane materials as well as the minimum temperature that they would need to be heated to drive off the ammonia for regeneration.

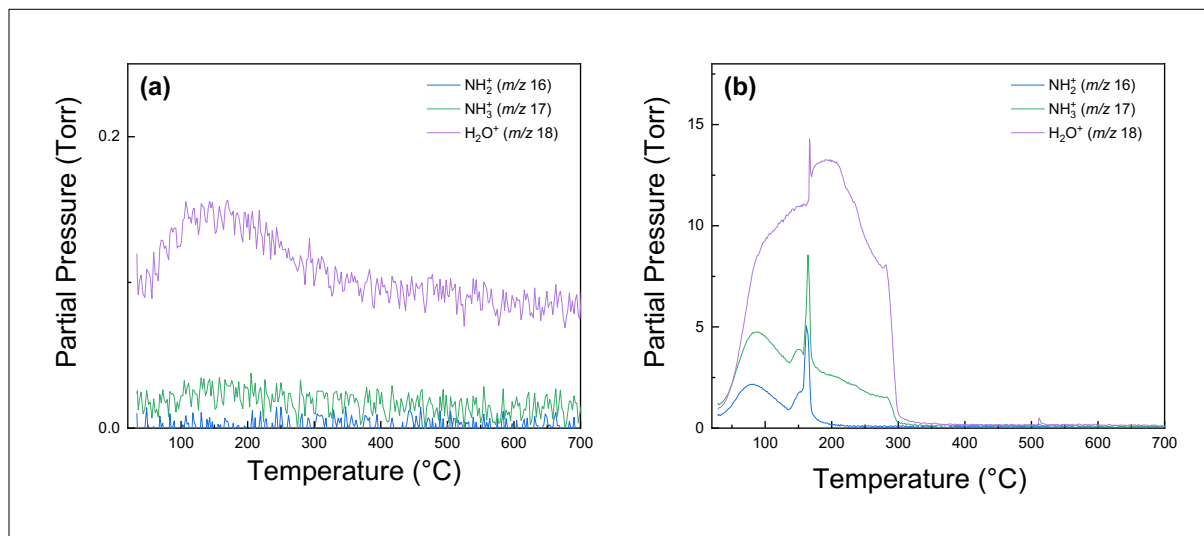


Figure 3-12. TPD for GO (a) as is and (b) with ammonia

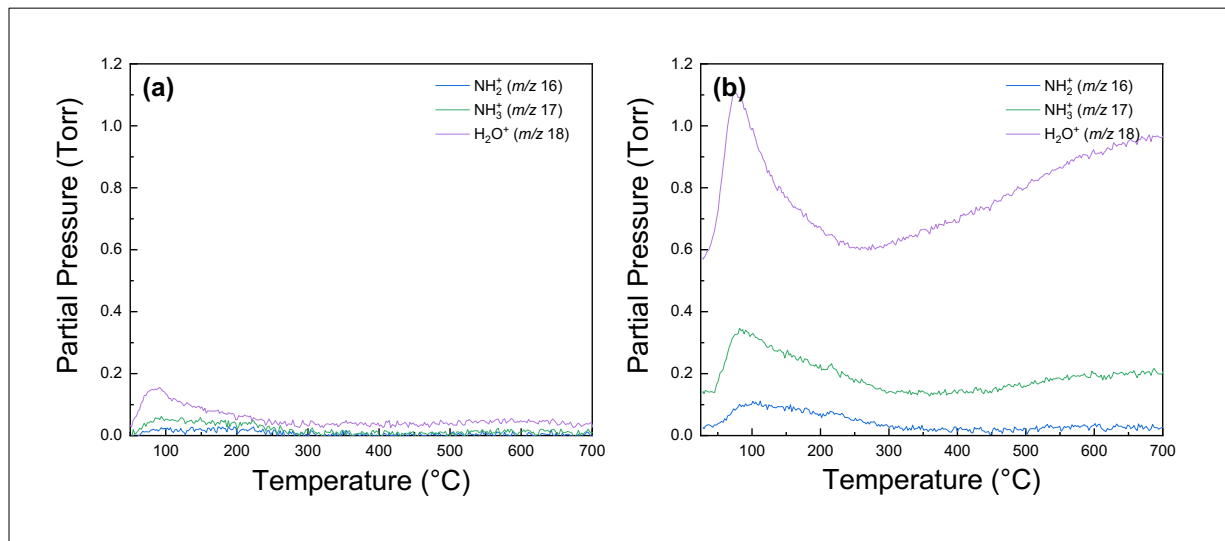


Figure 3-13. TPD for BN (a) as is and (b) with ammonia

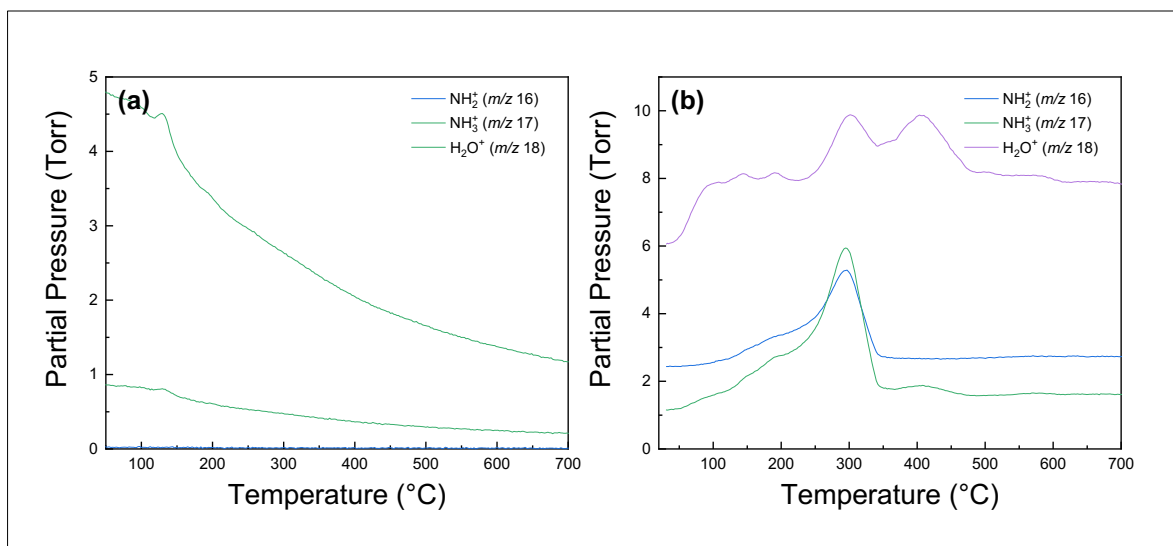


Figure 3-14. TPD for MoS₂ (a) as is and (b) with ammonia

4.0 Conclusions

Membranes composed of porous, two dimensional layered structures were successfully created and tested in different gas streams. Graphene oxide-based membranes appeared to have the best performance, with the lowest concentration of ammonia measured on the outlet of the membrane. All the membranes appeared to have slightly lower nitrogen permeation after several ammonia permeation runs, indicating a slight loss of the porous structure; however, this effect was minimal.

5.0 Recommendations, Path Forward or Future Work

This data shows the potential for these membranes to be used in line to moisture probes with further development. To improve these materials, more in-depth studies of the interactions between the ammonia and the membranes should be studied as a route to develop more robust, longer lasting membranes. TPD results show the ammonia can be driven off with temperature and could lead to the ability for the membranes to be regenerated; however, the effect of heat treatment on the membrane performance would need to be investigated. The effect of tritiated compounds in the gas stream on the membrane stability and lifetimes should also be measured.

6.0 References

1. Chen, Z.; Lu, C., Humidity Sensors: A Review of Materials and Mechanisms. *Sensor Letters* **2005**, *3* (4), 274-295.
2. Khanna, V. K., A plausible ISFET drift-like aging mechanism for Al₂O₃ humidity sensor. *Sensors and Actuators B: Chemical* **2015**, *213*, 351-359.
3. Heiranian, M.; Farimani, A. B.; Aluru, N. R., Water desalination with a single-layer MoS₂ nanopore. *Nature Communications* **2015**, *6* (1), 8616.
4. Kim, H. W.; Yoon, H. W.; Yoon, S.-M.; Yoo, B. M.; Ahn, B. K.; Cho, Y. H.; Shin, H. J.; Yang, H.; Paik, U.; Kwon, S.; Choi, J.-Y.; Park, H. B., Selective Gas Transport Through Few-Layered Graphene and Graphene Oxide Membranes. *Science* **2013**, *342* (6154), 91-95.
5. Wang, L.; Boutilier, M. S. H.; Kidambi, P. R.; Jang, D.; Hadjiconstantinou, N. G.; Karnik, R., Fundamental transport mechanisms, fabrication and potential applications of nanoporous atomically thin membranes. *Nature nanotechnology* **2017**, *12* (6), 509-522.
6. Bunch, J. S.; Verbridge, S. S.; Alden, J. S.; van der Zande, A. M.; Parpia, J. M.; Craighead, H. G.; McEuen, P. L., Impermeable Atomic Membranes from Graphene Sheets. *Nano Letters* **2008**, *8* (8), 2458-2462.
7. Deng, M.; Kwac, K.; Li, M.; Jung, Y.; Park, H. G., Stability, Molecular Sieving, and Ion Diffusion Selectivity of a Lamellar Membrane from Two-Dimensional Molybdenum Disulfide. *Nano Letters* **2017**, *17* (4), 2342-2348.
8. Li, H.; Song, Z.; Zhang, X.; Huang, Y.; Li, S.; Mao, Y.; Ploehn, H. J.; Bao, Y.; Yu, M., Ultrathin, Molecular-Sieving Graphene Oxide Membranes for Selective Hydrogen Separation. *Science* **2013**, *342* (6154), 95-98.
9. Oyama, S. T.; Lee, D.; Hacırlıoğlu, P.; Saraf, R. F., Theory of hydrogen permeability in nonporous silica membranes. *Journal of Membrane Science* **2004**, *244* (1), 45-53.
10. Krishnamoorthy, K.; Veerapandian, M.; Yun, K.; Kim, S. J., New function of molybdenum trioxide nanoplates: Toxicity towards pathogenic bacteria through membrane stress. *Colloids and Surfaces B: Biointerfaces* **2013**, *112*, 521-524.

Appendix A.

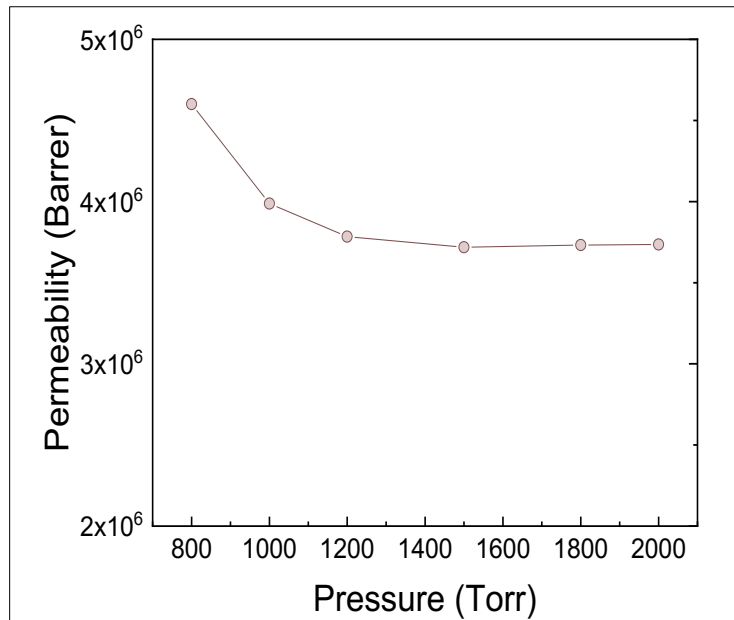


Figure A-1. Nitrogen permeability of a blank (unfunctionalized) filter paper membrane

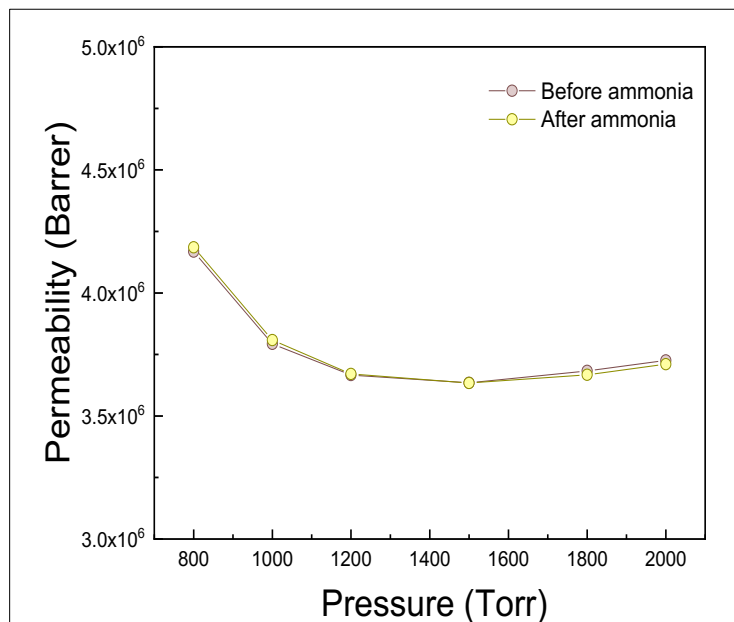


Figure A-2. Nitrogen permeability of a blank (unfunctionalized) membrane before and after ammonia permeation

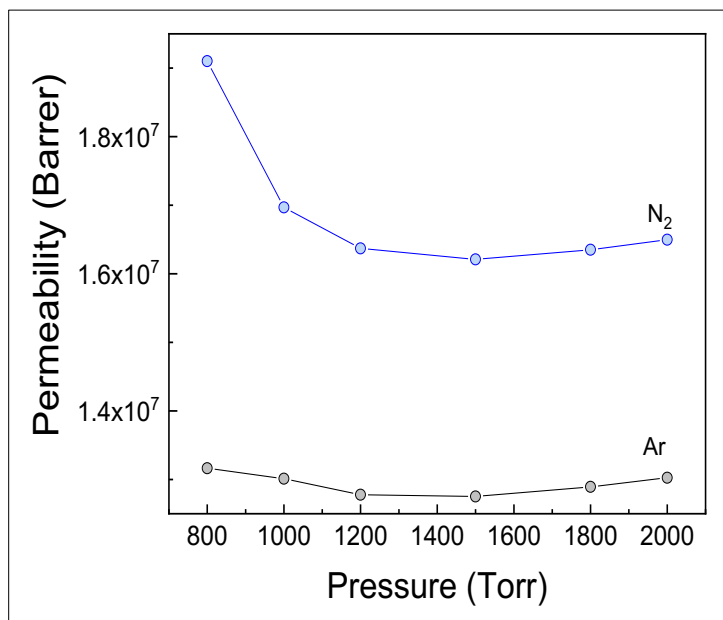


Figure A-3. Effect of gas size on permeability through MoO_3 membranes

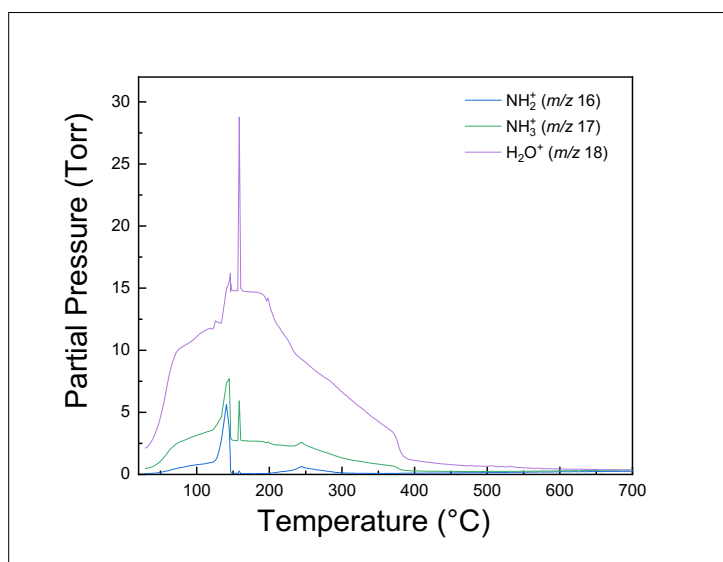


Figure A-4. TPD measurement of GO with ammonia

Distribution:

The standard distribution of all technical reports is:

alex.cozzi@srnl.doe.gov

david.crowley@srnl.doe.gov

c.diprete@srnl.doe.gov

a.fellinger@srnl.doe.gov

samuel.fink@srnl.doe.gov

nancy.halverson@srnl.doe.gov

erich.hansen@srnl.doe.gov

connie.herman@srnl.doe.gov

patricia.lee@srnl.doe.gov

Joseph.Manna@srnl.doe.gov

john.mayer@srnl.doe.gov

daniel.mccabe@srnl.doe.gov

Gregg.Morgan@srnl.doe.gov

frank.pennebaker@srnl.doe.gov

Amy.Ramsey@srnl.doe.gov

William.Ramsey@SRNL.DOE.gov

michael.stone@srnl.doe.gov

Boyd.Wiedenman@srnl.doe.gov

bill.wilmarth@srnl.doe.gov

Records Administration (EDWS)

Paul Foster
Davis Cyr
Heather Mentzer
Paul Beaumont
Jeffrey Steedley
Donna Allison